Time-lapse FWI using simultaneous sources

He. Liu*, Xin. Fu, Daniel. Trad, Kristopher. Innanen
he.liu1@ucalgary.ca

To overcome the challenge of expensive computational costs for FWI process, shot subsampling methods and source-encoding strategies have been used to make the full waveform inversion efficient while maintaining the quality of the inversion results with minimum sacrifice. In this work, we incorporate amplitude-encoding strategy with cyclic subsampled data scheme, which first subsamples the data cyclically and then compose blended during the iterations. In this way, we can directly eliminate much more crosstalk terms introduced by encoded individual shot gathers and reduce the data dimension to improve FWI efficiency.

SUBSAMPLING THE SHOTS

Cyclic subsampling method that uses every shot the same number of times or at least a similar number of times (Fig 1). To avoid distance variability between the selected shots, the selected shots in each subgroup are uniformly spaced.

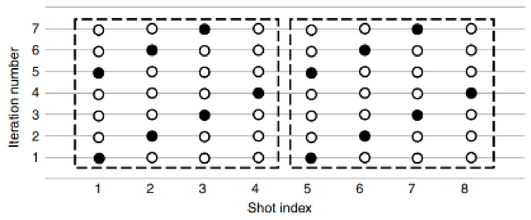

Fig 1. The cyclic subsampling scheme, the black dots indicate the shots used in an iteration (adopted from Ha and Shin, 2013).

AMPLITUDE-ENCODING SCHEME

In amplitude-encoding FWI, shot gathers are transformed into super shot gathers by the encoding matrix, which is defined as

$$\mathbf{B} = \begin{bmatrix} b^{1,1} & \dots & b^{Nsig,1} \\ \vdots & \ddots & \vdots \\ b^{1,N_{sup}} & \dots & b^{Nsig,N_{sup}} \end{bmatrix}_{N_{sup} \times N_{sig}} .$$

SYNTHETIC EXAMPLES

Acoustic Marmousi model

We subsample 58 shot gathers to compose 10 super-shots with even spatial distance from all 174 shots and re-subsample the data cyclically every a few iterations. From the crosstalk matrix comparison, we can notice many off-diagonal elements are reduced to zero.

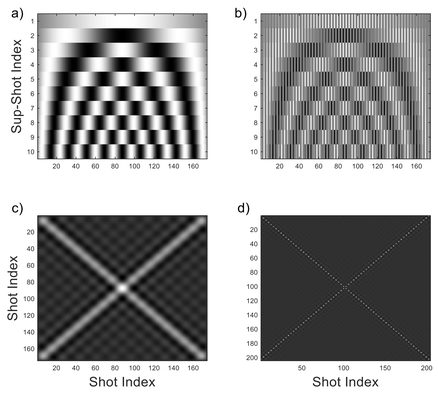

Fig 2. The encoding (first row) and crosstalk (second row) matrices: using all the individual shots (left column) and subsampled shots (right column).

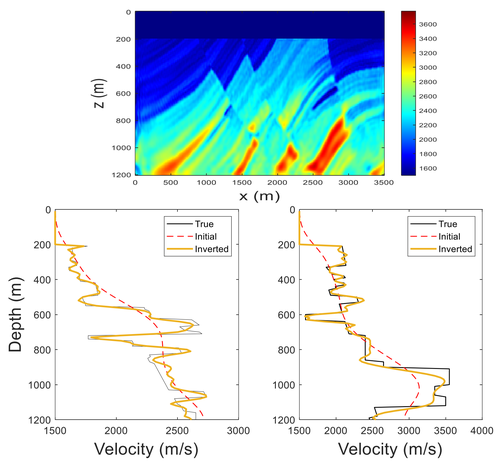

Fig 3: Inverted baseline model and its vertical profiles.

From inverted baseline and monitor models, we can see there introduces no obvious crosstalk noises in the final images. Using parallel time-lapse FWI strategy, we use the same scheme to invert the monitor model, which is shown in Fig 4b., we obtain the inverted time-lapse model after subtraction, shown in Fig 4c. we can see the well inverted velocity changes in the two reservoirs.

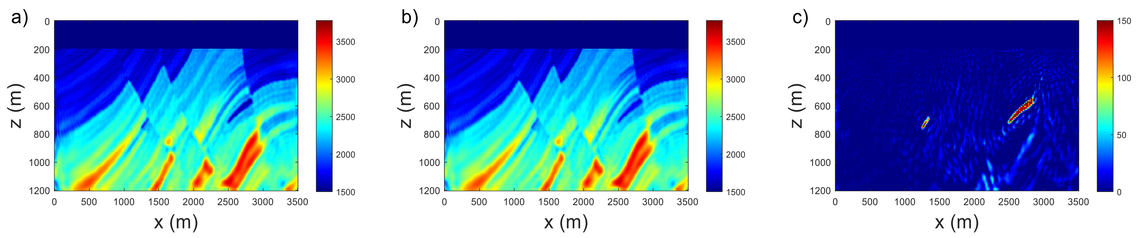

Fig 4: Inverted baseline, monitor and time-lapse models.

Elastic Marmousi model

In this experiment, we subsample every 3 shots and compose 40 super-shots. For elastic FWI, we use a multi-scale approach and invert baseline and monitor models from 1 Hz to 20 Hz. Also, we first present the inversion results for baseline model. The final images and vertical profiles of vp and vs at two velocity change areas are shown in Fig 6 and Fig 7, respectively.

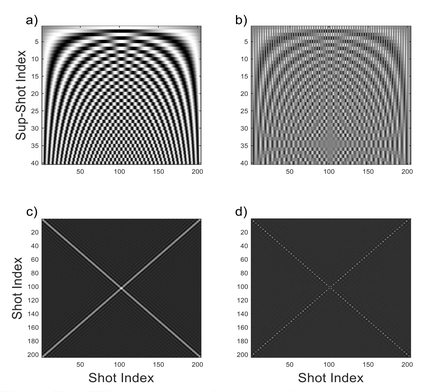

Fig 5: The encoding (first row) and crosstalk (second row) matrices.

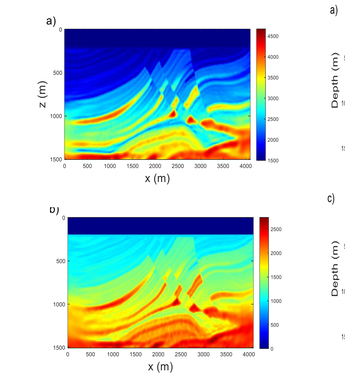

Fig 6. Inverted baseline model, a) vp and b) vs.

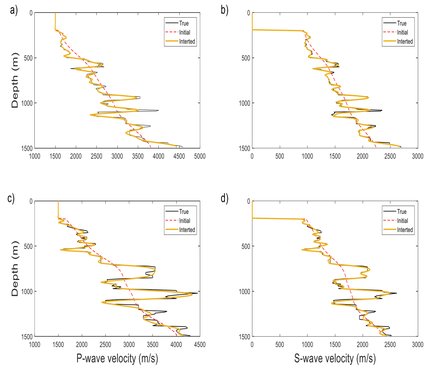

Fig 7: Vertical profiles at distance 2.1 km and 3.0 km: a) and c) P-wave velocity, b) and d) S-wave velocity.

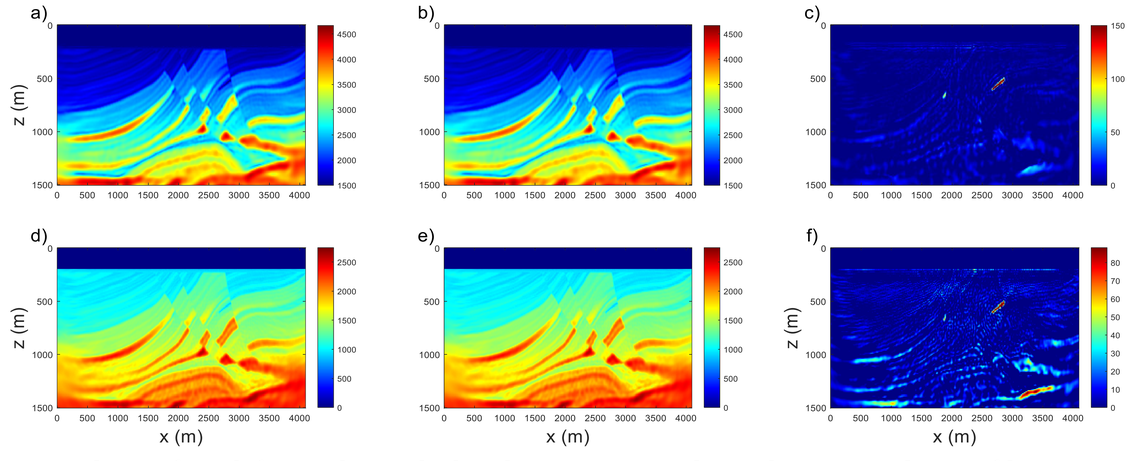

Fig 8. Columns from left to right are the baseline, monitor and time-lapse vp and vs profiles.

CONCLUSTIONS

We presented cyclic subsampled data-based amplitude-encoding time-lapse FWI in time domain. FWI examples show that using amplitude-encoding with subsampled shots can make the inversion process efficient with minimum sacrifices in the inversion results.

We have applied this scheme to both acoustic and elastic time-lapse FWI, both synthetic examples show promising results.

NSERC CRSNG
UNIVERSITY OF CALGARY
FACULTY OF SCIENCE
Department of Geoscience